



# Effect of DCSBD plasma treatment distance on surface characteristics of wood and thermally modified wood

R. Talviste<sup>1</sup> · O. Galmiz<sup>2</sup> · M. Stupavská<sup>2</sup> · J. Ráhel<sup>2</sup>

Received: 26 October 2019 / Published online: 8 April 2020  
© Springer-Verlag GmbH Germany, part of Springer Nature 2020

## Abstract

This study focused on plasma treatment of European beech (*Fagus sylvatica*) and heat-treated European beech surfaces with varying distance from the planar electrode of the diffuse coplanar surface barrier discharge. In addition to the treatment in the air, plasma treatment was also carried out in O<sub>2</sub>, CO<sub>2</sub>, N<sub>2</sub> and Ar atmospheres. Treatment was differentiated between treatment in the active plasma zone and in the so-called plasma afterglow region. Air plasma treatment in the active plasma zone led to the well-known improvement of surface wettability of polar liquids due to increased polar part of surface free energy. Treatment in plasma afterglow region caused the wettability decline of polar liquids and caused a more hydrophobic surface. The phenomenon was primarily present for air plasma treatment. Oxygen-to-carbon ratio measured by X-ray photoelectron spectroscopy did not change with the treatment in air plasma afterglow. Based on additional tests with pure cellulose paper and based on findings in previous studies, the reason for increased hydrophobicity was suggested to be degradation of hemicelluloses on the wood surface.

## Introduction

Typically, atmospheric pressure plasma treatment of wood (Sakata et al. 1993; Odrášková et al. 2008; Wolkenhauer et al. 2008, 2009; Gerullis et al. 2018), polymeric materials (Liston et al. 1993; Kormunda et al. 2012) or glass (Homola et al. 2013) surfaces results in an increased surface free energy (SFE) and enhanced wetting (i.e., hydrophilicity) by polar liquids such as water. Recently, it was observed that the effect of wood plasma treatment mediated by diffuse coplanar

---

✉ R. Talviste  
rasmus.talviste@ut.ee

<sup>1</sup> Institute of Physics, University of Tartu, W. Ostwaldi tn 1, 50411 Tartu, Estonia

<sup>2</sup> Department of Physical Electronics, Masaryk University, Kotlarska 2, 60137 Brno, Czech Republic

surface barrier discharge (DCSBD) depends strongly on the distance between the treated surface and the DCSBD electrode (Tino and Smatko 2014; Jablonsky et al. 2016). Plasma treatment at distances up to 0.4 mm creates a more hydrophilic wood surface, whereas at distances above 0.6 mm, the water contact angle increases, i.e., the surface becomes more hydrophobic. The origin of this effect is still unclear.

Atmospheric pressure plasmas such as DCSBD are cold plasmas operated at close to room temperature. The main benefit for material surface modification arises from interactions with plasma-generated active species such as electrons, ions, excited neutral species and ultraviolet radiation. The lifetimes of active species vary over many orders of magnitude and determine which species are present in different situations, for example, in active plasma zone or in the afterglow. Reactions involving electrons occur on the timescale of several to tens of nanoseconds, chemistry of excited neutral species occurs within milliseconds timescale and some of the long-lived species such as O<sub>3</sub> and NO<sub>x</sub> species (NO, NO<sub>2</sub>, NO<sub>3</sub> and N<sub>2</sub>O<sub>5</sub>) have lifetimes up to several seconds (Eliasson et al. 1994; Wagner et al. 2003; Sakiyama et al. 2012).

The increased hydrophilicity of wood after plasma treatment is generally explained by the increased polar part of SFE (Mahlberg et al. 1998; Wolkenhauer et al. 2008, 2009; Peters et al. 2017). The X-ray photoelectron spectroscopy (XPS) analysis has revealed that the cause for increased polar part of SFE is an increase in the surface oxygen-to-carbon atomic ratio (O/C ratio) (Belgacem et al. 1995; Wascher et al. 2014; Altgen et al. 2016; Gerullis et al. 2018). At the same time, however, a short duration DCSBD treatment (Gerullis et al. 2018; Galmiz et al. 2019; Talviste et al. 2019) or DBD treatment (Altgen et al. 2016) does not change the wood surface morphology.

Therefore, it is reasonable to assume that the increase in hydrophobicity observed previously (Tino and Smatko 2014) at larger treatment distance but short treatment duration is caused by some changes in surface chemistry or composition. One possible hypothesis for the increased hydrophobicity is that the polar part of SFE decreases, for example, due to a decrease in O/C ratio.

Wood is a complex natural material composed primarily of cellulose, lignin, hemicelluloses and extractives. Thermally, modification of wood is modification of wood in a process of partial pyrolysis in a low-oxygen atmosphere. It results in increased durability due to alteration of chemical structures of the components of the cell wall (Tjeerdsma and Militz 2005; Gérardin et al. 2007). In essence, thermal modification causes degradation of hemicelluloses and cellulose, which provides an increase in the relative lignin content. It has been previously shown that plasma can differently affect model substances of cellulose and lignin (Klarhöfer et al. 2010). Air plasma treatment resulted in oxidation and increased O/C ratio of lignin, whereas the model compound of cellulose, cellobiose, was on the contrary chemically reduced and exhibited a lower O/C ratio (Klarhöfer et al. 2010). Thus, a possible explanation for increased hydrophobicity could be that plasma treatment has different effects on individual wood components at varying distances.

In the already mentioned works (Tino and Smatko 2014; Jablonsky et al. 2016), only the water contact angle was used to characterize the wood surface after DCSBD plasma treatment. However, no explanation was suggested for the cause of

the increased water repellency at larger distances in those works. The aim of this work is to address this deficiency. The surfaces of beech and thermally modified beech wood samples were characterized after a short time DCSBD treatment at varying distances by SFE measurements and XPS analysis. The focus was to characterize and explain the increased hydrophobic character of wood surfaces after treatment at larger distances, i.e., in the plasma afterglow. Furthermore, the effect of plasma forming gas on the wood surface characteristics was studied by a pair comparison of treatments in  $N_2$ ,  $O_2$ ,  $CO_2$  and Ar atmospheres.

## Materials and methods

### Plasma treatment setup

Wood samples were treated by diffuse coplanar surface barrier discharge (DCSBD) (Hoder et al. 2008; Černák et al. 2009; Stepanova et al. 2017). The experimental setup is shown in Fig. 1. The DCSBD electrode system consists of 32 parallel strip-line silver electrodes (1.5 mm wide, 220 mm long with 1 mm gap between strips) embedded in 96% alumina ceramics. The closed reactor chamber allowed to create plasma in air, Ar,  $N_2$ ,  $CO_2$  and  $O_2$  atmospheres. Prior to the treatment in a gas atmosphere other than air, the reactor was flushed for 5 min at a flow rate of 5 slm. Plasma treatment was then carried out at a flow rate of 1 slm. Experiments in air were performed in ambient air atmosphere. The electrode system was powered by an AC voltage (15 kHz and 20 kV peak-to-peak) at a fixed power of 400 W except for Ar, where 200 W was used due to the occurrence of arcing at higher power inputs. About 90% of the total power was deposited in the discharge plasma (Stepanova et al. 2017). The treatment time was fixed to 10 s in all experiments.

The thickness of the thin active plasma layer in the DCSBD device was identified as the zone where the majority of excitation/ionization process occurs and was

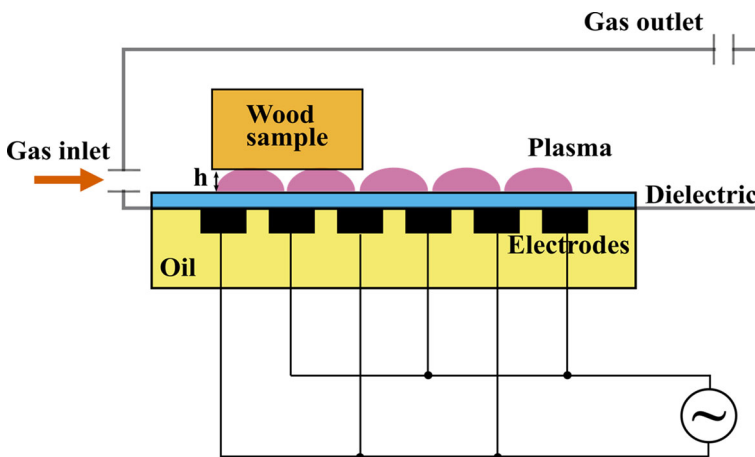


Fig. 1 Schematic of the DCSBD setup

determined spectroscopically to be approximately 0.3 mm (Stepanova et al. 2017). The distance between the DCSBD planar electrode and surface of the wood sample was investigated as the first parameter affecting surface modification. Glass microscope slides (0.15 or 1 mm thick) were used to set three distinct distances: 0.15 mm located inside the active discharge zone, 0.45 mm just above the active discharge and 1 mm located further away in the afterglow region.

### Thermally modified wood samples

In addition to the treatment distance, the maximum pyrolysis temperature of European beech (*Fagus sylvatica*) was investigated as the second parameter. Heat treatment of all samples was carried out in the Department of Wood Science at the Mendel University of Brno. A closed pilot reactor was used for treatment in an atmosphere composed of 80% of water vapor and 20% of air. The temperature was increased at a constant rate of 0.42 °C/min until the treatment temperature of 160, 180 or 200 °C was reached, which was then kept constant for 3 h.

Thermally treated samples were planed and cut into the final dimensions (20 × 20 × 100 mm<sup>3</sup> radial–tangential–longitudinal) and stored in a storage box with controlled relative humidity for a minimum of 2 weeks. Relative humidity of 55% at 20 °C was achieved using a saturated solution of magnesium nitrate Mg(NO<sub>3</sub>)<sub>2</sub> × 6H<sub>2</sub>O in distilled water (Wexler and Hasegawa 1954). The density of beech and beech heat-treated at 160, 180 and 200 °C was measured to be 730, 700, 650 and 655 kg/m<sup>3</sup>.

### Surface free energy determination

The indirect determination of surface free energy and its polar and dispersive components was done using the Owens–Wendt regression method (Wendt and Owens 1969). Four liquids were used in this study: distilled water ( $\gamma^D = 21.9$  mN/m,  $\gamma^P = 51$  mN/m), ethylene glycol ( $\gamma^D = 29$  mN/m,  $\gamma^P = 19$  mN/m), diiodomethane ( $\gamma^D = 50.8$  mN/m,  $\gamma^P = 0$  mN/m) and glycerol ( $\gamma^D = 28.3$  mN/m,  $\gamma^P = 36.9$  mN/m) (Gindl et al. 2001). A surface energy evaluation system (Advex Instruments, Czech Republic) was used to measure contact angles (CA) directly from the ICCD camera images. CAs of 15 droplets (1 µl) were measured for each testing liquid, and the average values were used for the Owens–Wendt regression. CAs were determined at the point when the wetting rate becomes constant ( $d\theta/dt = \text{const}$ ) (Nussbaum 1999).

### X-ray photoelectron spectroscopy

X-ray photoelectron spectroscopy (XPS) measurements were taken on an ESCALAB 250Xi (Thermo Fisher Scientific, East Grinstead, United Kingdom). An X-ray beam with a power of 200 W (650 µm<sup>2</sup> spot size) was used. The survey spectra were acquired with a pass energy of 50 eV and resolution of 1 eV. High-resolution scans were acquired with a pass energy of 20 eV and resolution of 0.1 eV. To compensate for the charges on the surface, an electron flood gun was used. Spectra were referenced to the hydrocarbon type C1s component set at a

binding energy of 284.8 eV. Spectra calibration, processing and fitting routines were done using Avantage software.

### **Additional experiments with UV radiation, long-lived species and cellulose paper**

The aim of these experiments was to determine to what extent the UV radiation and/or long-lived chemical species alone can deliver the observed increase in hydrophobicity at 1 mm distance. The DCSBD was operated at the standard experimental conditions given above.

To test the role of UV radiation, a thin UV transparent sapphire plate of 0.7 mm was placed at a height of 0.3 mm (directly above the active plasma layer) from the DCSBD electrode surface between the discharge plasma and the wood surface placed 1 mm above the electrode. The sapphire plate served as a mechanical barrier for transport of active chemical species but allowing generated UV radiation to pass through.

To test the role of long-lived species, the wood sample was placed in a closed reactor for 60 s and the side, which did not face the plasma electrode, was investigated. This setup excluded the influence of everything except for long-lived species with a rising concentration in the chamber during the 60 s. The surfaces treated in these selective treatment experiments were characterized by water CA measurements only.

Finally, pure cellulose filter paper ERT FF3 (Hollingsworth & Vose, USA) was treated in air with the DCSBD setup described above at the distance of 0 and 1 mm. The aim of this experiment was to determine whether the pure cellulose is susceptible to the hydrophobization by the remote plasma treatment. The cellulose paper was treated on both sides. The change in surface hydrophilicity was characterized by the Washburn capillary rise method (Kirdponpattara et al. 2013) by measuring the rate of water uptake by a vertically positioned cellulose paper strip of  $130 \times 10 \times 0.5 \text{ mm}^3$ , which was brought into level contact with the water surface.

## **Results and discussion**

### **Surface free energy and its components**

Figure 2 displays the polar and dispersive part of SFE for beech and thermal beech after 10 s of plasma treatment in air at varying distance from the DCSBD planar electrode. The shown uncertainty bars correspond to the standard deviation of the slope and intercept of the linear regression model fit and were in the range of 1–2 mJ/mm<sup>2</sup>. Total SFE of reference samples (no plasma treatment) showed a gradual reduction with growing thermal treatment temperature. Its polar part was the highest for native beech. Higher thermal treatment temperature caused its progressive reduction from 21.9 to 3.8 mJ/mm<sup>2</sup>. By contrast, the dispersive part of SFE of the reference samples (prior to plasma treatment) exhibited progressive

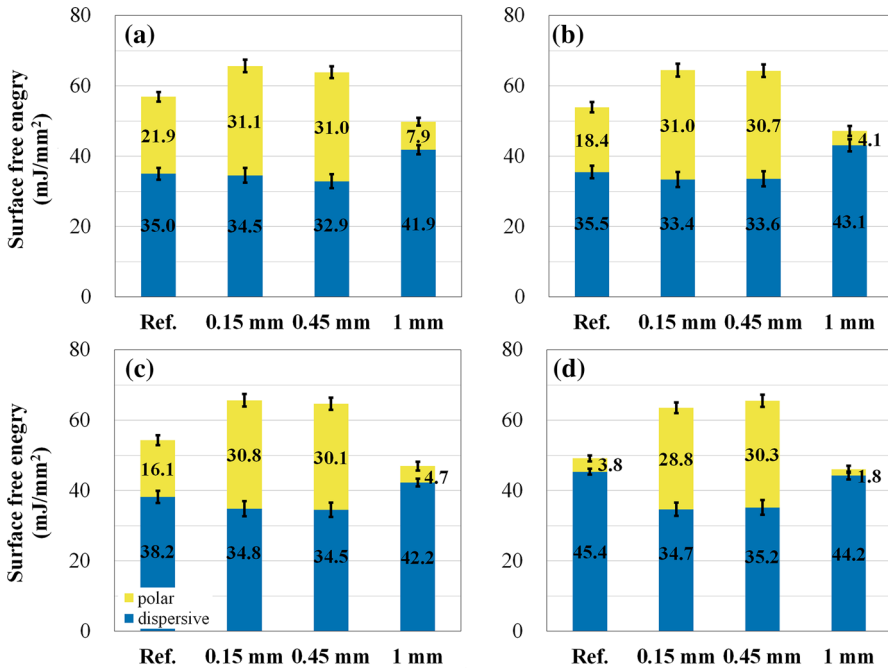


**Fig. 2** SFE components of native beech (a) and beech thermally treated at 160 °C (b), 180 °C (c), and 200 °C (d) after plasma treatment in air at varying distances from the DCSBD electrode. Reference (Ref.) indicates the sample prior to plasma treatment. Uncertainty bars correspond to the standard deviation of the slope and intercept of the linear regression

increase from 35.0 to 45.4 mJ/mm<sup>2</sup>. This is in accordance with previous works by Sansonetti et al. (2013) and Chu et al. (2016).

Plasma treatment at 0.15 and 0.45 mm resulted in increased SFE (up to 63–66 mJ/mm<sup>2</sup>) for all investigated samples. The polar component increased up to 29–31 mJ/mm<sup>2</sup>, which has already been explained by increased surface oxidation accompanied by higher values of O/C ratio (Altgen et al. 2016; Talviste et al. 2019). The dispersive part of native beech and beech heat-treated at 160 °C was not affected by plasma treatment. Beech heat-treated samples of 180 and 200 °C showed a decrease in the dispersive component similar to studies by Altgen et al. (2016) and Talviste et al. (2019).

Remote plasma treatment at 1 mm distance resulted in significantly lower total SFE (46–50 mJ/mm<sup>2</sup>) for all samples except for beech heat-treated at 200 °C, which showed the same values for both components of SFE as before plasma treatment. The polar part of SFE was reduced down to a few mJ/mm<sup>2</sup>. At the same time, the dispersive part increased up to 42–44 mJ/mm<sup>2</sup> except for 200 °C beech, where the change coincided within the calculated uncertainty. These results correspond well with the decrease in water CAs on similarly plasma-treated beech reported in Jablonsky et al. (2016).

The present measurements (Fig. 2) showed that regardless of the prior heat treatment temperature, plasma treatment at distances 0.15 mm and 0.45 mm

resulted in similar values of SFE (63–66 mJ/mm<sup>2</sup>) and their polar (29–31 mJ/mm<sup>2</sup>) and dispersive (33–35 mJ/mm<sup>2</sup>) components. Since the thickness of the DCSBD active plasma layer is 0.3 mm only, this indicates that for beech and heat-treated beech, the oxidizing effect of DCSBD plasma was sufficiently strong to achieve maximum surface oxidation and increased polar part of the SFE even when the treated surface was placed slightly above the active plasma layer. Interestingly, for oak at distances above 0.25 mm, the effect of wettability improvement measured by water uptake times was lost (Odráškova et al. 2008).

The main difference between the treatment in active plasma zone and plasma afterglow region is due to the composition of present plasma species. Plasma chemistry in air at atmospheric pressure occurs on timescales of several to tens of nanoseconds for electron chemistry and up to minutes for long-lived neutral species such as O<sub>3</sub> and NO<sub>x</sub> (Sakiyama et al. 2012). It is expected that in case of treatment inside the active zone (0.15 mm in the present case), the surface modification is achieved by combined contribution of ions, electrons, radicals, UV radiation and long-lived neutrals. In case of 1 mm treatment, the contribution of short-lived species should be minimal (Benard et al. 2008; Sakiyama et al. 2012). Therefore, the dominant species that reach the surface and cause the treatment effect are primarily long-lived neutrals such as O<sub>3</sub> and NO<sub>x</sub> and UV radiation. The short-lived radicals, electrons and ions are lost by recombination and do not reach the treated surface.

As pointed out in the introduction, water CA after short time DCSBD plasma treatment depends on the distance between the treated wood surface and DCSBD electrode (Jablonsky et al. 2016). The boundary where the treatment result has changed from more hydrophilic to more hydrophobic occurred at 0.4–0.5 mm depending on the wood species (Tino and Smatko 2014). The present results at 1 mm treatment (Fig. 2) clarify that the increased water CAs reported in that work (Tino and Smatko 2014) are a result of decreased polar part (and increased dispersive part) of SFE. In fact, the CAs of all polar liquids (water, ethylene glycol and glycerol) used in this work increased after the remote plasma treatment. Furthermore, the hydrophobization effect is present not only on native wood surfaces but also on wood heat-treated at temperatures up to 180 °C.

### XPS and O/C ratio

XPS analysis was focused on the remote plasma treatment at 1 mm, since the treatment in active plasma zone is already well-known to cause the increased O/C ratio (Altgen et al. 2016; Talviste et al. 2019). Figure 3 displays the O/C ratio for beech samples. Table 1 presents the deconvoluted components of the C1s peak for reference and plasma-treated samples. In addition to carbon and oxygen, the analyzed samples contained 1–2% of nitrogen both before and after plasma treatment.

The results showed that the surfaces of beech and beech heat-treated at 200 °C were oxidized (O/C ratio increased), while the observed change was within uncertainty for beech heat-treated at 160 and 180 °C. In any case, the increase in O/C ratio was substantially lower than that of active plasma treatment, where a more

**Fig. 3** O/C ratio of beech samples after 10 s plasma treatment in air at a distance of 1 mm. The shown values are an average of minimum three measurements, and uncertainty is given as the standard deviation. Ref. is reference sample before plasma treatment

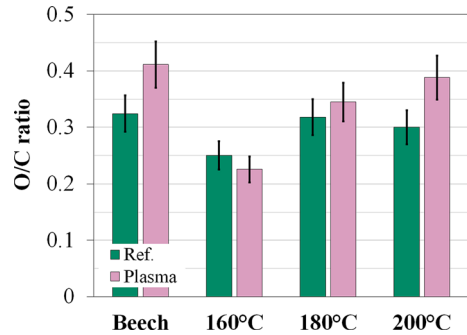


**Table 1** Components of the deconvoluted C1s peak of beech samples before (reference) and after plasma treatment of 10 s at 1 mm

C1s component	Beech		Beech 160 °C		Beech 180 °C		Beech 200 °C	
	Ref.	Plasma	Ref.	Plasma	Ref.	Plasma	Ref.	Plasma
C1	50.5	35.8	60.6	60.5	57.6	57.8	58.8	47.2
C2	35.3	42.3	32.1	27.1	34.3	30.8	36.5	36.6
C3	7.4	11.9	3.9	6.1	5.3	7.0	2.6	10.3
C4	6.8	10.0	3.5	6.3	2.8	4.4	2.0	5.9

The values given in the table are an average of three measurements, and the relative standard deviation was 20–25%

than twofold increase has been observed (Talviste et al. 2019). One possible explanation for increased O/C ratio of beech is degradation of extractives during the plasma treatment (Avramidis et al. 2012), which is supported by the decrease in the C1 component after plasma treatment (Table 1) assigned to extractives (Altgen et al. 2016). On the other hand, plasma oxidation is stronger with increased lignin content (Altgen et al. 2016). Higher heat treatment temperature is known to result in increased relative amount of lignin (Inari et al. 2006). Therefore, in case of beech heat-treated at 200 °C, the decrease in the C1 component and increase in O/C ratio after plasma treatment are likely related to more pronounced oxidation of lignin.

Several previous studies attributed the increased hydrophilicity of plasma-treated wood surfaces to the increased O/C ratio on the surface (Odrášková et al. 2008; Lux et al. 2013; Altgen et al. 2016). Here, the experiments showed (Fig. 2) that although the increased hydrophobicity can be explained by changes in the components of SFE, these changes are associated with only small variations in O/C ratios as measured with XPS (Fig. 3). In fact, the decrease in the polar part of SFE was also associated with a slight increase in O/C ratio, which contradicts the expected response that the amount of oxygen containing polar functional groups would decrease.



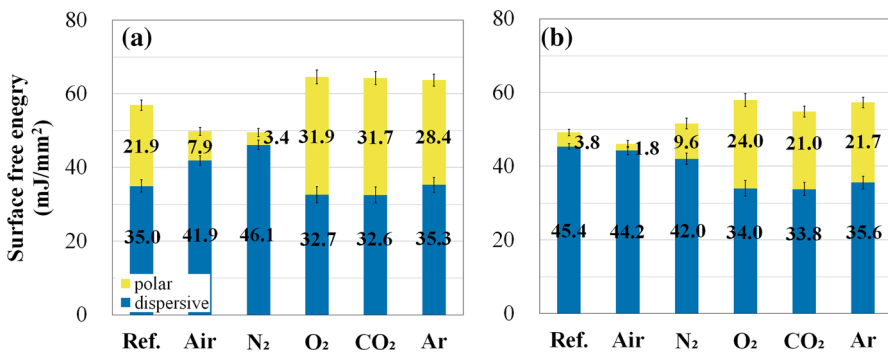
## Variation of plasma treatment atmosphere

Figure 4 displays the SFE components of beech and 200 °C heat-treated beech after 10 s of remote plasma treatment in various gas atmospheres at the distance of 1 mm from the DCSBD electrode. In the case of beech, plasma treatment in air and N<sub>2</sub> atmospheres resulted in decreased total SFE with decreased polar part and increased dispersive part. Thus, the air treatment's hydrophobization effect has been reproduced well.

Remote treatment in O<sub>2</sub>, CO<sub>2</sub> and Ar atmospheres increased the total SFE by increasing its polar part. Absolute values of SFE resulting from the remote treatment in O<sub>2</sub>, CO<sub>2</sub> and Ar were comparable to those obtained by air plasma treatment at small distances (i.e., 0.15 and 0.45 mm).

With respect to beech heat-treated at 200 °C, all atmospheres except for air resulted in higher SFE. Treatment in O<sub>2</sub>, CO<sub>2</sub> and Ar atmospheres gave more than a fivefold increase in polar part of SFE and some 20% reduction in its dispersive part. In N<sub>2</sub> atmosphere, only a minor increase in the polar part was observed. It should be noted, however, that N<sub>2</sub> plasma-treated samples exhibited an unexpectedly high standard deviation in measured CAs of water ( $60 \pm 16^\circ$ ), whereas typical contact angle standard deviations were in the range of  $\pm 5^\circ$ .

Unlike in air, remote treatment in Ar, O<sub>2</sub> and CO<sub>2</sub> resulted in improved surface wettability, due to significantly increased polar part of SFE. In O<sub>2</sub> and CO<sub>2</sub> plasmas, the predominant long-lived active species is ozone. Air and N<sub>2</sub> non-thermal plasmas are characterized by an ample presence of nitrogen oxides NO<sub>x</sub> such as NO, NO<sub>2</sub>, N<sub>2</sub>O, NO<sub>3</sub> and N<sub>2</sub>O<sub>5</sub> (Braun et al. 1988). In the case of pure N<sub>2</sub> gas, oxygen molecules needed for NO<sub>x</sub> formation originate most likely from water molecules adsorbed at the wood surface. The well-known presence of OH and NO $\gamma$  spectroscopic emission lines in inert (oxygen-free) DBD plasmas is generally attributed to surface reactions with adsorbed water (Bibinov et al. 2001). Remote treatment in air and pure N<sub>2</sub> rendered beech surface more hydrophobic. However, this does not necessarily mean that NO<sub>x</sub> causes the surface hydrophobization



**Fig. 4** SFE components of native beech (a) and beech heat-treated at 200 °C (b) after remote plasma treatment of 10 s at 1 mm in various gaseous atmospheres. Ref. is reference sample before plasma treatment

directly. The presence of  $\text{NO}_x$  reduces the concentration of  $\text{O}_3$ , which could slow down the surface oxidation. In air and  $\text{N}_2$  plasmas, several additional loss channels exist for ozone, which is connected either with oxidation of  $\text{NO}_x$  into higher oxides (Sakiyama et al. 2012), or hamper the ozone formation by consuming forming atomic oxygen; and these losses are not present in  $\text{O}_2$  and  $\text{CO}_2$  plasmas. These reactions include for example



where M is a third collision partner (e.g.,  $\text{O}_2$  or  $\text{N}_2$  in air). Experimentally, the concentration of ozone was measured in surface barrier discharge arrangement to reach up to 2000 ppm in pure oxygen (Simek et al. 2010), while in the air, a maximum value of 800 ppm was measured inside the active plasma zone (Jōgi et al. 2017). According to Jōgi et al. (2017), the ozone concentration at 1 mm is around 500 ppm. The XPS measurements showed an increased O/C ratio on beech surfaces after plasma treatment at 1 mm in  $\text{O}_2$  and  $\text{CO}_2$  plasmas by 0.1 compared to reference samples, which is comparable to the increase in O/C ratio in air (Fig. 3). Plasma treatment in  $\text{O}_2$  and  $\text{CO}_2$  resulted in increased polar part (and decreased dispersive part) after treatment at 1 mm, and determining the reason of this effect would require further studies.

The cause of surface oxidation after the treatment in Ar plasma can be explained by reactions with fragments of adsorbed water molecules, dissociated by highly energetic excited Ar atoms or by secondary oxidation after the radical sites at the wood surface created by argon plasma are exposed to ambient laboratory air. Increased O/C ratio of cellulose has been observed after inert Ar plasma treatment (Kolarova et al. 2013). Klarhöfer et al. (2010) observed a decreased O/C ratio after Ar plasma treatment of lignin and model compound for cellulose. However, in that work, plasma treatment was carried out in the same chamber as the photoelectron spectroscopic analysis and, therefore, secondary oxidation when the sample is brought into contact with ambient air can be excluded.

Separate extended treatments with UV or exposure to long-lived species did not result in changes within the experimental uncertainty in the CA values. For native beech, initial CA of  $37 \pm 6^\circ$  was (un)changed to  $42 \pm 7^\circ$  upon both types of exposure. For beech heat-treated at  $200^\circ\text{C}$ , initial CA of  $72 \pm 7^\circ$  was (un)changed to  $77 \pm 7^\circ$  and  $80 \pm 7^\circ$  for UV and long-lived species treatment, respectively. Thus, the increased wood surface hydrophobicity after plasma treatment at 1 mm could not be caused by exposure to only UV radiation or long-lived species, which could indicate that more complicated processes occur on the surface that require both UV radiation and long-lived active species (e.g.,  $\text{O}_3$  and  $\text{NO}_x$ ). However, this would require further studies.

## Pure cellulose paper

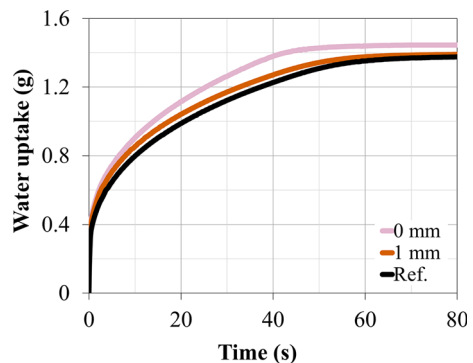
Figure 5 displays the water uptake of tested cellulose paper with time. Each uptake curve is an average of five measurements. The standard deviation of maximum values was taken as the measurement uncertainty. Compared to the reference sample, plasma treatment at 0 mm resulted in faster uptake of water and higher total water uptake. The reference sample adsorbed in total  $1.37 \pm 0.03$  g in about 70 s, while the sample exposed to plasma treatment inside the active discharge saturated at  $1.44 \pm 0.02$  g in about 50 s, which indicates that direct plasma treatment at 0 mm rendered cellulose paper more hydrophilic as was the case with beech wood (Fig. 2). For remote plasma treatment at 1 mm, the total water uptake of  $1.39 \pm 0.04$  g was practically the same as that of a reference sample and occurred in about 65 s (i.e., minor change from 70 s of the untreated sample), which proves that remote plasma treatment has a negligible effect on the wetting characteristics of pure cellulose material.

## Possible cause of increased hydrophobicity at 1 mm plasma treatment

The plasma effect on specific wood components has been highlighted in several studies (Klarhöfer et al. 2010; Jamali and Evans 2011; Avramidis et al. 2012; Altgen et al. 2016). The present experiments with cellulose paper showed that the remote plasma treatment at 1 mm did not provide any significant change in neither the water uptake time nor in the total water uptake (Fig. 5), suggesting that the remote plasma modification of cellulose itself is minimal and should be disregarded as the cause for observed increased wood hydrophobicity.

Electron spectroscopy has shown that during plasma treatment the model compound for cellulose, cellobiose, was reduced primarily, whereas lignin was oxidized (Klarhöfer et al. 2010). Lignin is reported to be the most resistant wood component toward plasma etching (Jamali and Evans 2011). The authors have conclusively shown (Fig. 2) that the highest increase in polar part of SFE occurred for beech heat-treated at 200 °C (which expectedly contains the highest relative amount of lignin) when plasma-treated at 0.15 and 0.45 mm. Lignin seems to be very responsive to the treatment by short-lived plasma species. On the other hand,

**Fig. 5** Water uptake of cellulose paper as a function of time before (Ref.) and after 10 s of plasma treatment at a distance of 0 and 1 mm. Each uptake curve is an average of five measurements



the very same lignin-rich samples were practically inert to the remote treatment. Thus, the possibility of lignin alternation being responsible for the remote plasma hydrophobization can be safely excluded. Depending on treatment time, plasma treatment has been shown to fully degrade wood extractives (Avramidis et al. 2012). However, degradation of extractives would increase the hydrophilicity of the wood surface not decrease it.

The final wood components to consider are hemicelluloses. Hemicelluloses are amorphous molecules forming hydrogen bonds with polar liquids such as water and are smaller in size compared to cellulose. Hemicelluloses are known to degrade during the heat treatment of wood (Gérardin et al. 2007), which is regarded as the primary cause of increased hydrophobicity of thermally modified wood. It is possible that hemicelluloses on the surface are similarly degraded during the remote short duration plasma treatment, which may be the cause of the increased hydrophobicity of wood surfaces. The fact that beech heat-treated at 200 °C did not exhibit any hydrophobization effect nor any change of SFE (Fig. 2) supports this assumption because the hemicelluloses are expected to be substantially degraded on the surface after such high thermal treatment temperature (Alén et al. 2002).

Ozone has been argued to be the cause of increased plasma oxidizing effect on thermally modified wood compared to native wood (Altgen et al. 2016). In the coplanar barrier discharge, ozone concentration has been measured to decrease with distance from the electrode surface (Jögi et al. 2017). In case of plasma treatments at 0.15 and 0.45 mm, the hydrophobization effect due to the hemicellulose degradation is outcounted by far more intense surface oxidation by short-lived plasma species as is evident from increased O/C ratio (Altgen et al. 2016; Talviste et al. 2019) and the resulting effect is increased SFE.

## Conclusion

Diffuse coplanar surface barrier discharge in air, O<sub>2</sub>, CO<sub>2</sub>, Ar and N<sub>2</sub> atmospheres and varying distance from the planar electrode was applied for surface treatment of European beech (*Fagus sylvatica*) and heat-treated beech. The known effect of increased water contact angle after treatment at larger distances was shown to be caused by increased dispersive and decreased polar part of surface free energy. It was concluded that the degradation of hemicelluloses on the wood surface is the cause for this phenomenon. The hemicelluloses degradation is present at all distances from planar electrode. However, at smaller distances, it is effectively counteracted by the hydrophilization effect of short-lived plasma-generated species. Their absence at larger distances allows the hydrophobization effect to come forward. It was also found that the hydrophobization phenomenon occurs only when air and N<sub>2</sub> plasma is used. Treatment at 1 mm in O<sub>2</sub>, CO<sub>2</sub> and Ar plasma increased the polar part of SFE as well as total SFE.

**Acknowledgements** This work was supported by the Estonian Research Council (Grant No. PUTJD732) and Project LO1411 (NPU I) funded by the Ministry of Education, Youth and Sports of Czech Republic. We would also like to thank the Department of Wood Science at the Mendel University in Brno for providing the thermally treated wood samples.

## Compliance with ethical standards

**Conflict of interest** On behalf of all authors, the corresponding author states that there is no conflict of interest.

## References

- Alén R, Kotilainen R, Zaman A (2002) Thermochemical behavior of Norway spruce (*Picea abies*) at 180–225 °C. *Wood Sci Technol* 36:163–171. <https://doi.org/10.1007/s00226-001-0133-1>
- Altgen D, Avramidis G, Viöl W, Mai C (2016) The effect of air plasma treatment at atmospheric pressure on thermally modified wood surfaces. *Wood Sci Technol* 50:1227–1241. <https://doi.org/10.1007/s00226-016-0856-7>
- Avramidis G, Klarhöfer L, Maus-Friedrichs W, Militz H, Viöl W (2012) Influence of air plasma treatment at atmospheric pressure on wood extractives. *Polym Degrad Stab* 97:469–471. <https://doi.org/10.1016/j.polyimdegradstab.2011.12.030>
- Belgacem M, Czeremuskin G, Sapiéha S (1995) Surface characterization of cellulose fibres by XPS and inverse gas chromatography. *Cellulose* 2:145–157
- Benard N, Balcon N, Moreau E (2008) Electric wind produced by a surface dielectric barrier discharge operating in air at different pressures: aeronautical control insights. *J Phys D Appl Phys* 41:042002. <https://doi.org/10.1088/0022-3727/41/4/042002>
- Bibinov NK, Fateev AA, Wiesemann K (2001) On the influence of metastable reactions on rotational temperatures in dielectric barrier discharges in He-N<sub>2</sub> mixtures. *J Phys D Appl Phys* 34:1819–1826. <https://doi.org/10.1088/0022-3727/34/12/309>
- Braun D, Kühler U, Pietsch G (1988) Behaviour of NO<sub>x</sub> in air-fed ozonizers. *Pure Appl Chem* 60:741–746
- Černák M, Černáková L, Hudec I, Kováčik D, Zahoranová A (2009) Diffuse coplanar surface barrier discharge and its applications for in-line processing of low-added-value materials. *Eur Phys J Appl Phys* 47:22806. <https://doi.org/10.1051/epjap/2009131>
- Chu D, Xue L, Zhang Y, Kang L, Mu J (2016) Surface characteristics of poplar wood with high-temperature heat treatment: wettability and surface britleness. *BioResources* 11:6948–6967. <https://doi.org/10.15376/biores.11.3.6948-6967>
- Eliasson B, Egli W, Kogelschatz U (1994) Modelling of dielectric barrier discharge chemistry. *Pure Appl Chem* 66:1275–1286. <https://doi.org/10.1351/pac199466061275>
- Galmiz O, Talviste R, Kováčik D, Panáček R (2019) Cold atmospheric pressure plasma facilitated nanostructuring of thermally modified wood. *Wood Sci Technol* 53:1339–1352. <https://doi.org/10.1007/s00226-019-01128-6>
- Gérardin P, Petrič M, Petrisans M, Lambert J, Ehrhardt JJ (2007) Evolution of wood surface free energy after heat treatment. *Polym Degrad Stab* 92:653–657. <https://doi.org/10.1016/j.polyimdegradstab.2007.01.016>
- Gerullis S, Kretzschmar BS, Pfuch A et al (2018) Influence of atmospheric pressure plasma jet and diffuse coplanar surface barrier discharge treatments on wood surface properties: a comparative study. *Plasma Process Polym* 15(10):1800058. <https://doi.org/10.1002/ppap.201800058>
- Gindl M, Sinn G, Gindl W, Reiterer A, Stanzl-Tschegg S (2001) A comparison of different methods to calculate the surface free energy of wood using contact angle measurements. *Colloids Surf* 181:279–287
- Hoder T, Íra M, Kozlov KV, Wagner HE (2008) Investigation of the coplanar barrier discharge in synthetic air at atmospheric pressure by cross-correlation spectroscopy. *J Phys D Appl Phys* 41:35212–35219. <https://doi.org/10.1088/0022-3727/41/3/035212>
- Homola T, Matoušek J, Kormunda M, Wu LYL, Černák M (2013) Plasma treatment of glass surfaces using diffuse coplanar surface barrier discharge in ambient air. *Plasma Chem Plasma Process* 33:881–894. <https://doi.org/10.1007/s11090-013-9467-3>
- Inari NG, Petrisans M, Lambert J, Ehrhardt JJ, Gérardin P (2006) XPS characterization of wood chemical composition after heat-treatment. *Surf Interface Anal* 38:1336–1342. <https://doi.org/10.1002/sia.2455>
- Jablonsky M, Smatko L, Botkova M, Tino R, Sima J (2016) Modification of wood wettability (European beech) by diffuse coplanar surface barrier discharge plasma. *Cellul Chem Technol* 50:41–48

- Jamali A, Evans PD (2011) Etching of wood surfaces by glow discharge plasma. *Wood Sci Technol* 45:169–182. <https://doi.org/10.1007/s00226-010-0317-7>
- Jögi I, Erne K, Levoll E, Stamate E (2017) Radical production efficiency and electrical characteristics of a coplanar barrier discharge built by multilayer ceramic technology. *J Phys D Appl Phys* 50:aa8db. <https://doi.org/10.1088/1361-6463/aa8db>
- Kirdponpattara S, Phisalaphong M, Newby BZ (2013) Washburn capillary rise for determining contact angles of powders/porous materials. *J Colloid Interface Sci* 397:169–176. <https://doi.org/10.1016/j.jcis.2013.01.033>
- Klarhöfer L, Viöl W, Maus-Friedrichs W (2010) Electron spectroscopy on plasma treated lignin and cellulose. *Holzforschung* 64:331–336. <https://doi.org/10.1515/HF.2010.048>
- Kolarova K, Vosmanska V, Rimpelova S, Svorcik V (2013) Effect of plasma treatment on cellulose fiber. *Cellulose* 20:953–961. <https://doi.org/10.1007/s10570-013-9863-0>
- Kormunda M, Homola T, Matousek J, Kovacic D, Cernak M, Pavlik J (2012) Surface analysis of poly(ethylene naphthalate) (PEN) films treated at atmospheric pressure using diffuse coplanar surface barrier discharge in air and in nitrogen. *Polym Degrad Stab* 97:547–553. <https://doi.org/10.1016/j.polymdegradstab.2012.01.014>
- Liston EM, Martinu L, Wertheimer MR (1993) Plasma surface modification of polymers for improved adhesion: a critical review. *J Adhes Sci Technol* 7:1091
- Lux C, Szalay Z, Beikircher W, Kovacic D, Pulker HK (2013) Investigation of the plasma effects on wood after activation by diffuse coplanar surface barrier discharge. *Eur J Wood Prod* 71:539–549. <https://doi.org/10.1007/s00107-013-0706-3>
- Mahlberg R, Niemi HEM, Denes F, Rowell RM (1998) Effect of oxygen and hexamethyldisiloxane plasma on morphology, wettability and adhesion properties of polypropylene and lignocellulosics. *Int J Adhes Adhes* 18:283–297. [https://doi.org/10.1016/S0143-7496\(98\)00007-4](https://doi.org/10.1016/S0143-7496(98)00007-4)
- Nussbaum RM (1999) Natural surface inactivation of Scots pine and Norway spruce evaluated by contact angle measurements. *Holz Roh-Werkst* 57:419–424. <https://doi.org/10.1007/s001070050067>
- Odrášková M, Ráhel' J, Zahoranová A, Tino R, Černák M (2008) Plasma activation of wood surface by diffuse coplanar surface barrier discharge. *Plasma Chem Plasma Process* 28:203–211. <https://doi.org/10.1007/s11090-007-9117-8>
- Peters F, Hünnekens B, Wieneke S, Militz H, Ohms G, Viöl W (2017) Comparison of three dielectric barrier discharges regarding their physical characteristics and influence on the adhesion properties on maple, high density fiberboards and wood plastic composite. *J Phys D Appl Phys* 50:475206. <https://doi.org/10.1088/1361-6463/aa8fad>
- Sakata I, Morita M, Tsuruta K, Morita K (1993) Activation of wood surface by corona treatment to improve adhesive bonding. *J Appl Polym Sci* 49:1251–1258. <https://doi.org/10.1002/app.1993.070490714>
- Sakiyama Y, Graves DB, Chang HW, Shimizu T, Morfill GE (2012) Plasma chemistry model of surface microdischarge in humid air and dynamics of reactive neutral species. *J Phys D Appl Phys* 45:425201. <https://doi.org/10.1088/0022-3727/45/42/425201>
- Sansonetti E, Andersons B, Biziks V, Grinins J, Chirkova J (2013) Investigation of surface properties of hydrothermally modified soft deciduous wood. *Int Wood Prod J* 4:122–127. <https://doi.org/10.1179/2042645312Y.0000000028>
- Simek M, Pekarek S, Prukner V (2010) Influence of power modulation on ozone production using an AC surface dielectric barrier discharge in oxygen. *Plasma Chem Plasma Process* 30:607–617. <https://doi.org/10.1007/s11090-010-9245-4>
- Stepanova V, Kellar J, Galmiz O et al (2017) Areal homogeneity verification of plasma generated by diffuse coplanar surface barrier discharge in ambient air at atmospheric pressure. *Contrib Plasma Phys* 57:182–189. <https://doi.org/10.1002/ctpp.201600093>
- Talviste R, Galmiz O, Stupavska M, Tucekova Z, Kaarna K, Kovacic D (2019) Effect of DCSBD plasma treatment on surface properties of thermally modified wood R. *Surf Interfaces* 16:8–14. <https://doi.org/10.1016/j.surfin.2019.04.005>
- Tino R, Smatko L (2014) Modifying wood surfaces with atmospheric diffuse coplanar surface barrier discharge plasma. *Wood Fiber Sci* 46:459–464
- Tjeerdsma BF, Militz H (2005) Chemical changes in hydrothermal treated wood: FTIR analysis of combined hydrothermal and dry heat-treated wood. *Holz Roh-Werkst* 63:102–111. <https://doi.org/10.1007/s00107-004-0532-8>

- Wagner HE, Brandenburg R, Kozlov KV, Sonnenfeld A, Michel P, Behnke JF (2003) The barrier discharge: basic properties and applications to surface treatment. *Vacuum* 71:417–436. [https://doi.org/10.1016/S0042-207X\(02\)00765-0](https://doi.org/10.1016/S0042-207X(02)00765-0)
- Wascher R, Avramidis G, Vetter U et al (2014) Plasma induced effects within the bulk material of wood veneers. *Surf Coat Technol* 259:62–67. <https://doi.org/10.1016/j.surfcoat.2014.07.005>
- Wendt DK, Owens RC (1969) Estimation of the surface free energy of polymers. *J Appl Polym Sci* 13:1741–1747. <https://doi.org/10.1109/18.650986>
- Wexler A, Hasegawa S (1954) Relative humidity-temperature relationships of some saturated salt solutions in the temperature range 0° to 50°C. *J Res Natl Bur Stand* 53(1934):19–26
- Wolkenhauer A, Avramidis G, Militz H, Viöl W (2008) Plasma treatment of heat treated beech wood—investigation on surface free energy. *Holzforschung* 62:472–474. <https://doi.org/10.1515/HF.2008.074>
- Wolkenhauer A, Avramidis G, Hauswald E, Militz H, Viöl W (2009) Sanding vs. plasma treatment of aged wood: a comparison with respect to surface energy. *Int J Adhes Adhes* 29:18–22. <https://doi.org/10.1016/j.ijadhadh.2007.11.001>

**Publisher's Note** Springer Nature remains neutral with regard to jurisdictional claims in published maps and institutional affiliations.